A global assessment of wildfire potential under climate change utilizing Keetch-Byram drought index and land cover classifications

To cite this article: Colin S Gannon and Nik C Steinberg 2021 *Environ. Res. Commun.* **3** 035002

Environmental Research Communications

PAPER

A global assessment of wildfire potential under climate change utilizing Keetch-Byram drought index and land cover classifications

Colin S Gannon and Nik C Steinberg

Four Twenty Seven, Berkeley, California, United States of America

E-mail: cgannon@427mt.com

Keywords: wildfire, climate change, KBDI, land cover

Supplementary material for this article is available online

OPEN ACCESS

RECEIVED
17 July 2020

REVISED
17 December 2020

ACCEPTED FOR PUBLICATION
4 January 2021

PUBLISHED
6 April 2021

Abstract

In recent years, climate change has caused wildfires across the globe to generally become larger and more severe, creating new challenges for public health, housing and infrastructure, and natural resource management. As the characteristics of wildfires change, it is critical to understand where emerging risks for human and natural systems are most profound. We assess how future *wildfire potential*, defined here as the meteorological conditions and the availability of burnable vegetation types conducive to wildfire occurrence, are projected to change in the future. To achieve this, we combine modelled temperature and precipitation to calculate the Keetch-Byram Drought Index (KBDI) as a proxy for soil moisture deficit and overlay a weighting factor representing burnable vegetation derived from land cover classifications. Through our analysis of daily data at both mid- and end-of-century, we find that climate-related changes, such as increasing temperatures and drying patterns, will elevate wildfire potential globally, both in terms of severity of maximum daily KBDI and frequency of high KBDI days. We find that regions which have recently endured major fire events, including the western United States, Australia, and the Amazon, could experience increases in maximum KBDI of up to 100 in places, with more than 60 additional days of high KBDI by mid-century, compared to the historical baseline. Additionally, at the end-of-the-century, regions across much of Africa, Central America, and Southern Asia are projected to emerge as wildfire hotspots. While the occurrence of wildfires may still be rare today in many regions, we find that climatological trends are projected to increase wildfire potential for much of the globe, creating new risks for some, and raising the challenge for already wildfire-prone communities to effectively manage forests and protect people and critical resources.

1. Introduction

There has recently been a growing abundance of massive, severe wildfires across the globe, resulting in billions of dollars of direct and indirect damages, ecosystem and habitat destruction, public health impacts, and tragically, loss of life (Coogan *et al* 2019, Limaye *et al* 2019, French 2020). Climate change plays a major role in this trend (Abatzoglou and Williams 2016, Partain *et al* 2016, Kirchmeier-Young *et al* 2017, Herring *et al* 2018), and as the planet warms and precipitation patterns shift, it is generally expected that wildfire occurrence will increase and that fire seasons will lengthen for many areas of the world (Flannigan *et al* 2009). A lengthening wildfire season could spell trouble for places like California where the days with extreme fire weather has already more than doubled since the early 1980s (Goss *et al* 2020). To build resilience and inform decisions relevant to local fire management and preparedness, it is increasingly important not only to understand where wildfire exposure is the highest, but also which regions will experience significant changes in the meteorological conditions related to wildfire occurrence.

The occurrence and severity of any single wildfire, however, is determined by myriad factors, complicating the prediction of future events. Where and when a wildfire begins and its subsequent physical characteristics are dependent upon a few key variables: meteorological conditions, fuel sources, ignition sources, and, in many

cases, human activity (Flannigan *et al* 2009). While the actual occurrence of a wildfire and its characteristics after ignition will depend on many discrete factors, this paper will focus on *wildfire potential,* or the conditions which are conducive to wildfires, by evaluating select meteorological drivers and land cover classifications.

1.1. Meteorological drivers

Wildfires are a natural and often recurring phenomenon that play a central role in ecological processes across much of the world (Cochrane and Ryan 2009). Natural cycles in climate, ranging in timescales from seasonal to interdecadal, may heighten or diminish wildfire frequency and severity over time (Flannigan *et al* 2009) by bringing about periods of either hot and dry, or cool and wet weather. However, research indicates that an increasing trend in global fire activity and severity is partially attributable to climate change for many land cover types around the world, including fires in Alaska in 2015 (Partain *et al* 2016); British Columbia in 2017 (Kirchmeier-Young *et al* 2017); Australia in 2015–2016 (Herring *et al* 2018), and the western US over the last three decades (Abatzoglou and Williams 2016) These trends are elevating the potential for larger and more frequent wildfires due to the relationship between climate change and increased aridity (Williams *et al* 2019) and earlier spring snowmelt (Westerling *et al* 2006, Short 2014) driven by warmer temperatures. Additionally, there is evidence that fire seasons are lengthening in many regions, increasing the chances for wildfire occurrence. Notable examples of lengthening fire seasons include the western United States (Westerling *et al* 2006, Goss *et al* 2020), Spain, Portugal, and Italy (Jolly *et al* 2015). While sources of fire ignition and land use changes are significant contributors to the increase in global wildfire activity (Bowman *et al* 2009), climate change is overwhelmingly identified as the leading cause (Gillet *et al* 2004, Westerling *et al* 2006, Pechony and Shindell 2010, Abatzoglou and Kolden 2013, Williams *et al* 2019). Global circulation models (GCMs) are commonly used to explore the role of climate change in future wildfire extent, severity, and season length through variables such as temperature, precipitation, and humidity (Brown *et al* 2004, Liu *et al* 2010, Pechony and Shindell 2010, Kitzberger *et al* 2017). No study to-date has assessed the impact of climate change on future wildfire potential at a global level with such high temporal and spatial resolution as this study, while also utilizing a new generation of GCMs. We believe this level of granularity, which expands upon the findings of Liu *et al* (2010), is critical for risk accounting and planning, especially as wildfires grow more dangerous and begin to emerge in historically low risk environments.

Changes in the hydrological cycle related to climate change have contributed to multi-year droughts in many parts of the world (Cook *et al* 2015, Yoon *et al* 2015), which for many forested and dense vegetation types, leads to an abundance of dry fuels conducive to wildfire activity (van Mantgem *et al* 2009). Due to the relationship between aridity and fuel availability, soil moisture deficit, defined as the amount of water required to bring the soil to full saturation, has been widely used in wildfire indices to serve as a proxy for wildfire potential (e.g., Liu *et al* 2010) as wildfires tend to occur more frequently during periods of severe drought (Stephenson 1998, Westerling *et al* 2006, Dimitrakopoulos *et al* 2010).

1.2. Land cover

Land cover plays a critical role in wildfire behavior, as the predominant vegetation type of an area serves as a key fuel source and influences wildfire characteristics including frequency, intensity, and spread capacity (Cochrane and Ryan 2009). The exact characteristics of a fire will be significantly driven by the dryness and land management practices of the fuel sources in conjunction with other drivers, but the dominant vegetation type of an area can indicate the general level of burnability (Wahlberg *et al* 2014). Major wildfires occur across many different land cover types, ranging from coniferous (Thompson and Spies 2009) and deciduous forests (Li *et al* 2000) to grasslands and shrublands (Paysen *et al* 2000). Generally, the relationship between a specific land cover type and historical burned area is consistent across area (Forkel *et al* 2019), allowing for broad assessments of certain land cover types as they relate to wildfire globally.

1.3. Evaluating wildfire exposure

There is no consistent, generally agreed-upon metric for evaluating wildfire risk, due in large part to local differences in climate, soil, and vegetation types across the globe (Sommers *et al* 2011). Despite the usage of the term *wildfire risk*, probabilistic estimates lack the ability to precisely identify where and when wildfires could occur, and instead rely heavily upon decision-support frameworks, based largely on biophysical and meteorological conditions (Thompson and Calkin). The predictive power of probabilistic wildfire assessments has been somewhat limited due to the human variable, particularly with respect to wildfire ignition, which often determines where and when a fire will occur. Instead, many forward-looking fire outlooks use the term *wildfire potential*, as in this paper, to describe the conditions that are conducive to wildfires rather than to predict their actual occurrence (Liu *et al* 2010, Dillon *et al* 2015).

One such index which utilizes meteorological conditions to assess soil moisture deficit, a component of wildfire potential, is the Keetch-Byram Drought Index (KBDI) (Keetch and Byram 1968). KBDI is part of the United States' National Fire Danger Rating System and was designed to estimate the effect of soil moisture deficit on vegetation and, subsequently, wildfire potential in the southeastern United States. KBDI is calculated using precipitation and temperature variables to estimate evapotranspiration, and ranges from 0 to 800, or fully saturated soil to maximum soil moisture deficit, respectively.

The decision of which meteorological variables or indices to utilize for assessing future wildfire potential depends largely on the research question at hand. While not a direct measure of wildfire risk, KBDI is often used as a proxy for wildfire potential (Keetch and Byram 1968, Liu *et al* 2010, Taufik *et al* 2015). We selected KBDI because of its wide usage, global comparability, and compatibility with global climate models (GCMs). It is especially well-suited for global and forward-looking analyses that explore key, fire-related meteorological variables.

At least three operational systems actively use KBDI. The National Fire Danger Rating System (NFDRS) uses KBDI in conjunction with ignition and spread models to estimate the extent of dry fuel availability (Burgan et al 1998, Roads *et al* 2005); the United States Department of Agriculture's Forest Service uses it for research and warnings in the southeastern United States (Johnson and Forthum 2001); and the Australian states of Victoria, New South Wales and Queensland use it in an operational capacity to map levels of potential fire severity based on fuel dryness (Finkele *et al* 2006).

KBDI has also been applied to many other regions and land-cover types, including South Africa (Verbesselt *et al* 2006), Lebanon (Mitri *et al* 2015), the greater Mediterranean region (Dimitrakopoulos and Bemmerzouk 1998, Ganatsas *et al* 2011, Garcia-Prats *et al* 2015), Malaysia (Ainuddin and Ampun 2008), Hawaii (Dolling *et al* 2009), California (Yoon *et al* 2015), and globally to assess wildfire potential due to a changing climate (Liu *et al* 2010).

KBDI is suitable for describing fuel moisture content and wildfire spread after ignition because of its correlation with vegetation moisture across many land types (Dimitrakopoulos and Bemmerzouk 2003, Verbesselt *et al* 2006, Xanthopoulos *et al* 2006, Pellizzaro *et al* 2007). After investigating if KBDI is directly related to plant water stress in the Mediterranean, Xanthopoulos *et al* (2006) found that KBDI is a strong proxy of moisture deficit in soils, living plants, and dead organic matter, which may lend itself as a predictor of intense wildfire behavior. Several studies have also found there is a correlation between KBDI and burned area in other vegetation communities. Dolling *et al* (2009) found a strong relationship between fire activity across the Hawaiian Islands over a twenty-year period. Relationships between high KBDI and burned area have also been identified in the Western US (Abatzoglou and Kolden 2013, Abatzoglou and Williams 2016).

Each of these studies utilizes KBDI to approximate fuel dryness. Despite some of the physical assumptions (Chu *et al* 2002, Taufik *et al* 2015) and limitations (see *Limitations* section for more), KBDI is especially well-suited for evaluating future wildfire potential as it can be calculated using GCM projections of temperature and precipitation. The simplicity of the KBDI index, which keeps topographical and ecological parameters fixed, makes it a useful indicator for global analyses, especially when comparing meteorological conditions across different regions and timescales using GCMs.

Our assessment adapts the KBDI approach presented by Liu *et al* (2010) to assess wildfire potential on daily timesteps through the end of the century, allowing us to capture severity and frequency of KBDI extremes. (In this study, the term 'severity' is used to refer to conditions which could give rise to a wildfire, rather than to describe the characteristics of fires themselves). Unlike Liu *et al* (2010), we incorporate land cover types in our analysis, and build a weighting scheme based on historical wildfire occurrences as a means to represent fuel sources and determine the *burnability* of an area. With this approach, we are able project both absolute and relative differences of future wildfire potential in a world altered by climate change.

2. Data sources

For modeled precipitation and temperature variables, we use the ¼° degree statistically downscaled NASA Earth Exchange Global Daily Downscaled Projections (NEX-GDDP), derived from Coupled Model Intercomparison Project 5 (CMIP5) GCM output (Thrasher *et al* 2012). Our results are based on the multi-model mean of 18 models (see the *Climate models* section of the *supplementary materials* (available online at stacks.iop.org/ERC/3/035002/mmedia)) using the maximum daily temperature and total daily precipitation data variables under the Representative Concentration Pathway 8.5 (van Vuuren *et al* 2011), a scenario relevant from a risk and preparedness perspective. For land cover, we utilize the European Space Agency Climate Change Initiative (ESA CCI) Land Cover dataset (ESA 2017). This dataset renders the 2015 land cover type at approximately a 300-meter resolution across different classifications. We compare this against historical burned areas in the Collection 6 Moderate Resolution Imaging Spectrometer (MODIS) Burned Area product (Giglio *et al* 2018) to derive global

occurrence of fire activity within each land cover classification, and implement the findings from Kganyago and Shikwambana (2020) to associate ESA CCI land cover types with fire intensity. Additionally, we evaluate trends at a sub-regional level using the climate reference regions defined by Iturbide *et al* (2020) to aggregate each metric of wildfire potential to broader, climatologically consistent geographic regions (see the *Sub-region definitions* and *Sub-region results* sections of the *supplementary materials*).

3. Methods

We set out to evaluate future wildfire trends through an evaluation of wildfire potential. Our analysis does not attempt to indicate the likelihood that a fire will occur at a given location, but rather if the conditions are conducive to wildfire activity. Although the actual occurrence and characteristics of any individual fire depends heavily on the alignment of discrete variables, we focus our analysis on integrating fuel sources, based on land cover classification, with an index of soil moisture deficit (KBDI), to estimate the effect of climate change on wildfire potential globally.

3.1. Calculating Keetch-Byram drought index (KBDI)

We use modelled temperature and precipitation to calculate KBDI and evaluate vegetation dryness as it relates to wildfire potential. KBDI ranges from 0–800, where 0 indicates fully saturated soil, and 800 indicates the maximum soil moisture deficit, representative of 800 hundredths of an inch (i.e., 8 inches) of deficit.

$$Q_t = Q_{t-1} + dQ - dP \tag{1}$$

$$dQ = \frac{10^{-3}(800 - Q_{t-1})(0.968\, e^{0.0486T} - 8.3)\, dt}{1 + 10.88\, e^{-0.0441R}} \tag{2}$$

Here Q_t is the KBDI value on day t, Q_{t-1} is the KBDI of the previous day, dQ is the daily KBDI adjustment, and dP is the daily precipitation total. dQ is in turn a function of the daily maximum temperature (T), the average annual precipitation total (R), and the time increment (dt, one day for this application). We use an approach derived from Liu *et al* (2010) to evaluate KBDI in the historical baseline (1975 to 2005) and future time periods (*mid-century*, 2045 to 2055, and *end-of-century*, 2085 to 2095). The equations for KBDI take as inputs daily precipitation and daily maximum temperature, which are output from the NEX-GDDP product (see *Data Sources*). In equations (1) and (2), as in Liu *et al* (2010), we use a subset of years to build a climatological average year over which we iterate to allow KBDI values to spin-up to appropriate values and stabilize. We go one step further than Liu *et al* (2010) by using this spun-up climatological year to initialize our dataset, building in a run-up period of five years before calculating KBDI values for the years of interest in our historical baseline and projection period. See the *KBDI initialization and calculation* section of the *supplementary materials* for a more detailed description this approach.

These calculations result in KBDI daily values over a historical baseline and a projection time period. For each year in the projection period, we derive four metrics based on annual values to capture both future absolute and relative difference from the baseline over the dimensions of severity and frequency.

For measures of relative difference, the values reflect the differential of the future year of interest compared to the historical baseline average. For example, for the year 2050, we compare the maximum KBDI value to the annual average of the years 1975 to 2005. We then average each year in our projection period, e.g., 2045 to 2055, to arrive at our final relative difference metric value. Frequency of days with high wildfire potential relate to the KBDI scale breakdown presented in Liu *et al* (2010), where KBDI values in the 0–200 range are considered *low* risk, 200–400 *moderate*, 400–600 *high*, and 600–800 *extreme*. As such, any day with KBDI greater than or equal to 400 is counted as a high wildfire potential day and is the threshold for which we evaluate frequency of high KBDI days in this analysis.

3.2. Calculating burnability factor

Fuel sources play a vital role in fire behavior, dictating aspects of severity and rate of wildfire spread (Cochrane and Ryan 2009). As a proxy for identifying the extent of burnable area, we incorporate land cover classifications as a component of our assessment of wildfire potential. To do this, we assign a binned weighting factor to represent the *burnability* to each ESA CCI land cover classification (see the *Land cover classifications* section of the *supplementary materials*). To derive this weighting factor, we assess general, global trends in historical fire intensity and occurrence of wildfire within each land cover classification and combine them into a single burnability factor.

For intensity, we utilize the average maximum fire radiative power (FRP) across the regions evaluated in Kganyago and Shikwambana (2020). We normalize these values and assign intensity factor values of 1/3, 2/3, and 1 to the land cover classifications with normalized maximum FRP ranging from 0–1/3, 1/3–2/3, and

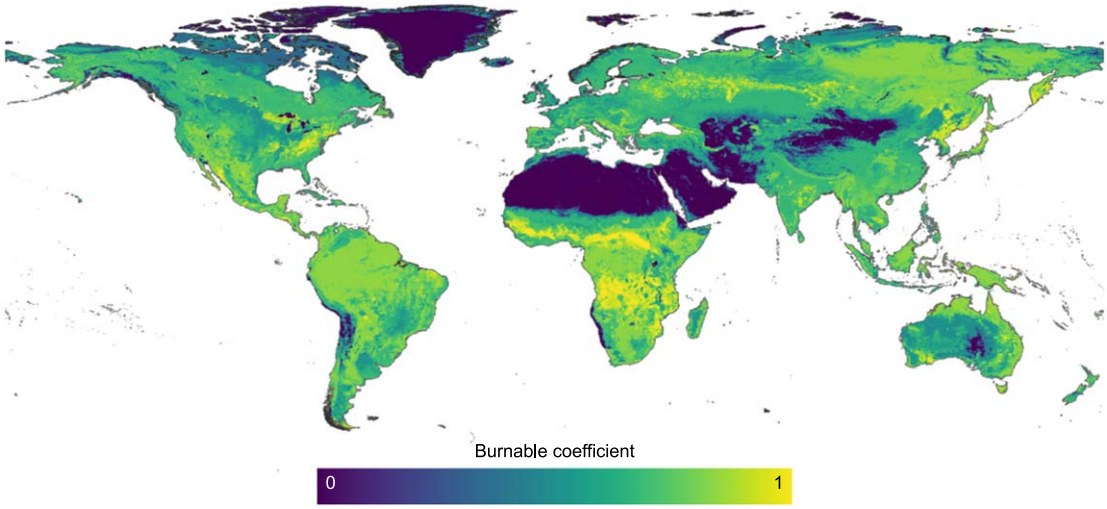

Figure 1. Upsampled land cover burnable coefficient, where 0 indicates no burnable land cover classifications within the 1/4° grid cell, and 1 indicates that all land cover classifications within the 1/4° grid cell have a high degree of burnability.

2/3–1, respectively. Additionally, since the land cover types presented in Kganyago and Shikwambana (2020) represent a grouping of multiple ESA classifications (e.g., 'forest cover' contains multiple ESA CCI land cover types associated with forests), the relevant intensity factor is mapped directly to the underlying land cover classifications within each grouping.

To represent occurrence of historical wildfire activity within land cover classification types, we implement the Collection 6 MODIS Burned Area product (Giglio *et al* 2018). We resample gridded burned area data from its 500-meter resolution to that of the ESA CCI land cover dataset (300-meter) to identify which ESA CCI grid cells have been identified as burned. We then consider two aspects of global fire activity: (1) the contribution of each land cover classification to total global burned area and (2) the proportion of each land cover classification which has burned. Averaging over all months from 2000–2020, we normalize both (1) and (2), average, and normalize again. From here, we assign a final binned weighting factor of 1/3, 2/3, and 1 based on the normalized values (see intensity factor derivation above), representing the fire occurrence weighting factor.

Finally, the average of the intensity factor and occurrence factor are averaged to arrive at a final burnability coefficient (table SM2), where zero represents no burnability and one represents a high degree of burnability. Certain classifications, such as water and urban areas, are excluded so that our assessment of burnability represents the pervasive vegetation types of the larger area and is not reduced by these land cover types. Remaining land cover types classified as non-vegetation in Kganyago and Shikwambana (2020) are by default assigned weighting factor scores of zero. By leveraging decades of satellite-based data of wildfire occurrence and intensity, we are able to broadly represent the burnability of different land classes, though recognize some vegetation communities may still not be fully represented in the findings. Caveats with this approach are further addressed in the *Limitations* section.

We then upsample ESA land cover weighting factors to the resolution of the climate models (1/4°). This is done by averaging the weighting factors for the land cover grid cells within each climate grid cell to arrive at a value for mean burnability, which is continuous from zero to one (figure 1). This value is used as a coefficient to represent available fuel sources and is referred to as the *burnable coefficient* within this paper.

3.3. Applying the burnable coefficient to KBDI metrics

To place the meteorological conditions associated with wildfire in the context of available fuels sources, we apply the burnable coefficient (figure 1) to the raw metrics of KBDI. Thus, the KBDI metrics derived from the climate models are adjusted based on the burnability of land cover classifications within each grid cell. For example, a location in the Sahara, which registers 800 for annual maximum KBDI, could be reduced to 0 after the coefficient is applied, since there is almost no burnable vegetation in the region, only bare area per the ESA CCI designation. In effect, most grid cells are discounted to better reflect wildfire potential based on availability of fuel sources in the area. These metrics with the burnable coefficient applied are referred to as the *adjusted* metrics throughout this paper and are denoted by the *adj* subscript.

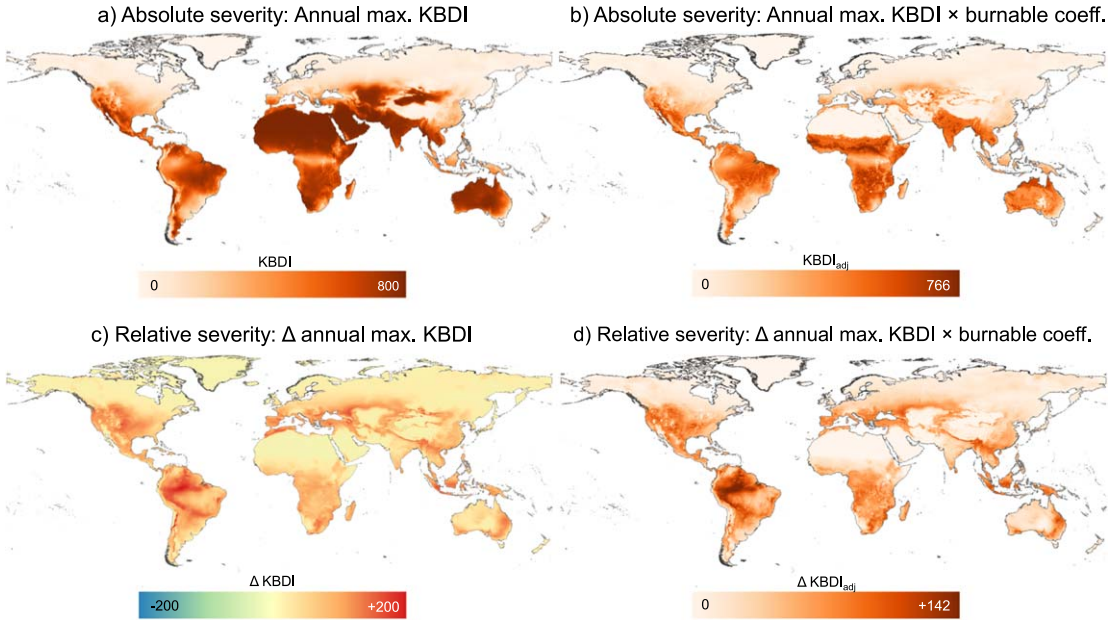

Figure 2. Mid-century wildfire potential severity. Map (a) indicates the raw annual maximum KBDI value, averaged across the years 2045–2055, (b) shows adjusted absolute severity, which was derived by applying the burnable coefficient to the raw values from map (a). Map (c) indicates differential 2045–2055 average annual maximum KBDI relative to the baseline, and map (d) shows the relative severity values from map (c) multiplied by the burnable coefficient.

3.4. Aggregation to sub-region level

To evaluate higher-level trends and compare across regions, we aggregate each adjusted KBDI metric to the sub-region level as defined by Iturbide *et al* (2020). To highlight the highest wildfire potential values within a sub-region, we identify the 95th percentile value of all grid cells within each sub-region for all four adjusted metrics (see the *Sub-region results* sections of the *supplementary materials*).

3.5. Evaluation of observed fire activity

To assess approximately how well our approach aligns with observed fire activity, we implement an assessment of fire frequency within each climate grid cell based on the MODIS burned area product. In this approach, we upsample the MODIS burned area product, counting the number of years in which a fire occurred within each climate grid cell. This observed data spanning from 2000–2020 effectively serves as a proxy for where fire activity has been the most common in the last 20 years. This is then compared to the modelled historical baseline (1975–2005) for *maximum* $KBDI_{adj}$ to assess correlation between our calculated wildfire potential values and observed fire occurrence.

4. Results

Our analysis produces four indicators of future wildfire potential: two based on absolute values of KBDI and two based on relative difference compared to the historical baseline, all with consideration for land cover burnability. Evaluating these adjusted metrics, we identify areas which exhibit the highest absolute and relative difference in wildfire potential during both mid- and end-of-century time periods. Figures 2 and 3 show raw and adjusted global maps for each metric at mid-century. Additionally, figure 4 highlights specific regions which exhibit higher values for each respective metric at end-of-century.

4.1. Absolute severity

Absolute severity is measured by the highest KBDI value (0–800) attained for each given location in a year, or the maximum soil moisture deficit at the peak of the wildfire season, averaged over the time period of interest. At mid-century, when evaluating raw absolute severity values (figure 2(a)), desert regions such as the Sahara, Arabian Peninsula, and central Australia, unsurprisingly approach the maximum possible KBDI value of 800. However, when burnable land cover classifications are factored in by applying the burnable coefficient (figure 1), many of these desert regions show little or no wildfire potential at mid-century due to lack of fuel sources (figure 2(b)). Consequently, it is the regions with a combination of high maximum KBDI and extensive burnable land cover which emerge with the highest *maximum* $KBDI_{adj}$. Semi-arid regions across the western United

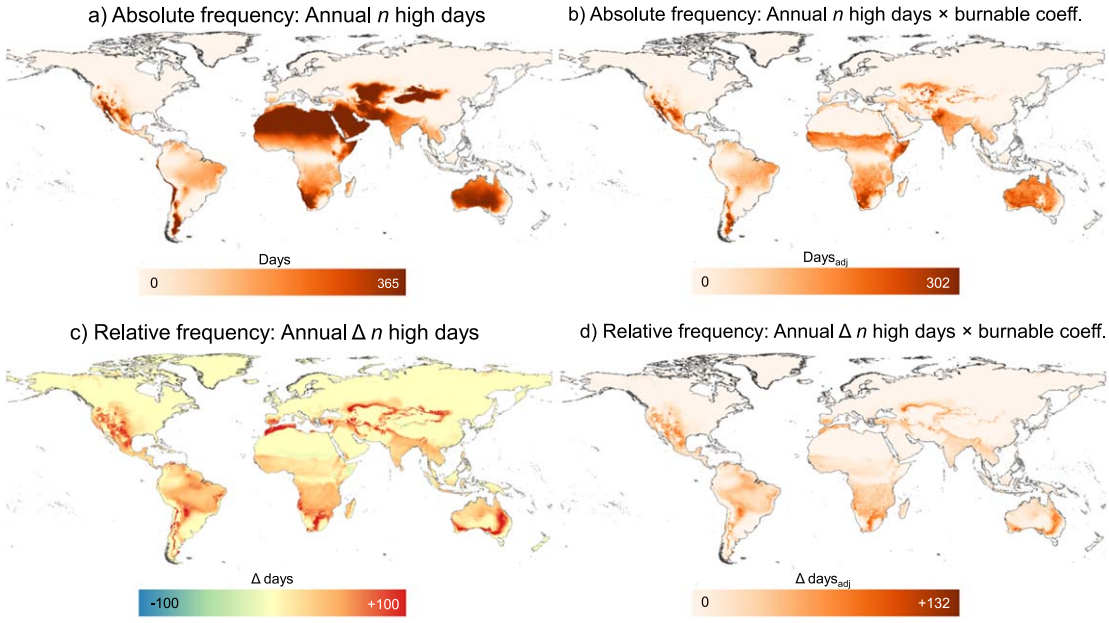

Figure 3. Mid-century wildfire potential frequency. Map (a) indicates the raw annual count of days where KBDI is above the high threshold (exceeds 400), averaged across the years 2045–2055, (b) shows adjusted absolute frequency, which was derived by applying the burnable coefficient to the raw values from map (a). Map (c) indicates differential 2045–2055 average annual count of high KBDI days relative to the baseline, and map (d) shows the relative frequency values from map (c) multiplied by the burnable coefficient.

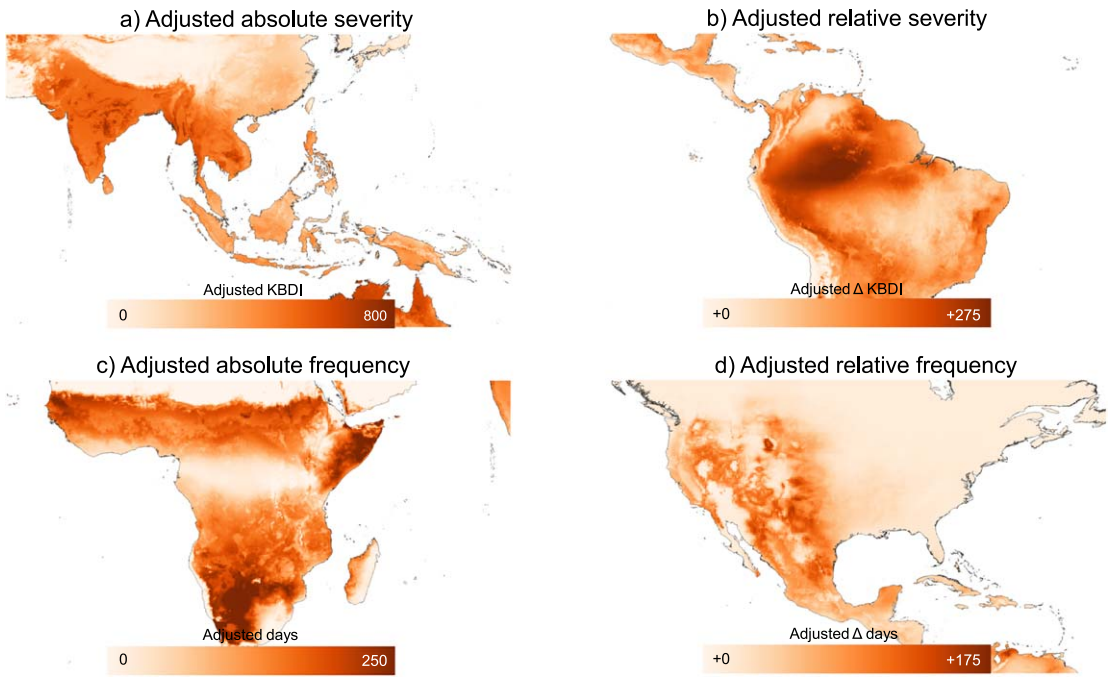

Figure 4. End-of-century (2085–2095) adjusted metric values, highlighting select hotspot regions. This map reflects the adjusted value (raw values with burnable coefficient applied) for the four metrics of wildfire potential absolute and relative severity and frequency.

States, Mexico, and northern Australia record high *maximum* $KBDI_{adj}$ values, as do subtropical and tropical regions including the Amazon rainforest, Central America, western and central Africa, and south-eastern Asia. At the sub-region level (see the *sub-region results* section of the *supplementary materials*), driven in part by the high volume and extent of burnable biomass, Central, West, South West, and North East Africa, along with Northern Central America and Northern Australia, are all among the sub-regions with the highest adjusted absolute severity at mid-century, each of which has a 95th percentile *maximum* $KBDI_{adj}$ value in excess of 600.

By the end of the century, we find the tropics, and to a lesser extent, the subtropics, continue to experience the highest absolute values for *maximum* $KBDI_{adj}$. We also find that *maximum* $KBDI_{adj}$ is projected to increase in

all sub-regions across the globe. All sub-regions in Africa outside of the Sahara have the highest *maximum* $KBDI_{adj}$ 95th percentile values globally at the end of the century, all of which exceed 660.

4.2. Relative severity

The relative severity metric highlights regions where the maximum KBDI value is significantly higher than the 1975–2005 baseline (figures 2(c) and (d)). Generally, the highest raw *changes in maximum KBDI* are evident in the tropics, including western portions of the Amazon and south-eastern Asia (figure 2(c)). There are noteworthy changes in the mid-latitudes as well, such as the continental US and central Asia. When considering land cover (figure 2(d)), northern latitudes in North America and Russia are further amplified, as are central Africa, the Amazon, and areas within southeast Asia. Among sub-regions, *change in maximum* $KBDI_{adj}$ between the baseline period and mid-century is most pronounced in South America, with the North, North Western, and Monsoon regions of the continent ranking as the three highest relative severity sub-regions globally. However high increases in *maximum* $KBDI_{adj}$ are also expected in other mid-latitude, subtropical, and tropical sub-regions as well, as evidenced by the 95th percentile values in Western and Central North America and Southern Asia all increasing by more than 90 $KBDI_{adj}$ over the baseline, representative of at least an 18% increase within each region.

We find that the largest *change in maximum* $KBDI_{adj}$ for the end of the century occurs in the northern areas of South America (figure 4(b)), inland areas just east of the Adriatic Sea, and Southeast Asia, especially Malaysia, Indonesia, and Papua New Guinea. Among sub-regions for *change in maximum* $KBDI_{adj}$, tropical and sub-tropical regions in South America and Africa are expected to remain hotspots, ranking among the highest values both at mid-century and end-of-century. Other notable sub-regions include the Mediterranean, Western and Central North America, Northern Central America, and Southeastern Asia, which all exhibit high 95th percentile *change in maximum* $KBDI_{adj}$, increasing by more than 160, or at least 34% respectively, by the end of the century.

4.3. Absolute frequency

The absolute frequency metric evaluates the average number of days per year when KBDI exceeds 400, which is considered high, as defined by Liu *et al* (2010). These high days represent times when the meteorological conditions evaluated in this study, temperature and precipitation, are particularly conducive to wildfire activity. As a result, areas such as in the Southwest US, western Amazon, southern Africa, and India may experience weeks or months where the wildfire potential is elevated (figure 3(a)). When evaluated with the burnable coefficient (figure 3(b)), more mid-latitude, subtropical, and equatorial regions show higher absolute frequency of wildfire potential. Broad areas of the tropics, such as much of India, and the non-equatorial regions of central and southern Africa, are all highly vegetated regions with a significant *number of high* $days_{adj}$. At the sub-region level, South West, Central and West Africa, Northern Central America, and Northern Australia could all experience exceptionally frequent occurrence of *high* $days_{adj}$. These sub-regions are all places where temperatures remain high year-round, and any extended period of precipitation deficit could be correlated with high fire risk.

By the end of the century, parts of subtropical central and southern Africa (figure 4(c)) are projected to experience well over 150 *high* $days_{adj}$ per year. Tropical sub-regions will continue to have the most elevated wildfire potential days by end-of-century, particularly in Northern Central America, South West and South East Africa. Northern Central America is expected to have the highest number of *high* $days_{adj}$ among all sub-regions with a 95th percentile value of 280 by end-of-century. Additionally, sub-regions including Central and Southern Australia, along with Southern Asia, will emerge as hotspots with elevated counts of *high* $days_{adj}$ at end-of-century.

4.4. Relative frequency

In addition to the absolute number of days with high KBDI, we also evaluate the difference in the number of high days relative to the baseline. This metric of change highlights regions which may have experienced a few or no high days in the 1975–2005 baseline but could experience more frequent high days in the future. The regions with the most notable increase in high days tend to be semi-arid regions, places where elevated wildfire conditions may already persist for a majority of the year but will subsequently extend to span the full year (figure 3(c)). When the burnable coefficient is applied (figure 3(d)), many of these semi-arid regions, including Central and Southern Australia remain hotspots, as the *change in number of high* $days_{adj}$ are among the highest globally. Northern Central America is projected to add the most *high* $days_{adj}$ with a 95th percentile increase of 70, or 33% higher than the historical baseline. Though less extensively burnable, parts of the sub-regions of South West and South East Africa are both projected to have more than 50 additional *high* $days_{adj}$ each by mid-century, representative of 32% and 51% increases, respectively, over the historical baseline.

By the end of the century, parts of Australia, southern Africa, Central and South America, and southern Europe are all projected to have a *change in high days*$_{adj}$ in excess of 60, a significant increase from the historical baseline, often well more than double the number of *high days*$_{adj}$ experienced in the past. In the southwestern United States, the *change in high days*$_{adj}$ is projected to rise by well over 100 additional days (figure 4(d)), representing several months' worth of additional elevated wildfire potential days. The sub-regions projected to experience the greatest *change in high days*$_{adj}$ by end-of-century span the globe with Northern Central America, South West and South East Africa, Southern Australia, and Western North America all expected to have a 95th percentile *change in high days*$_{adj}$ greater than 100 compared to the historical baseline, each with a relative increase in excess of 66%.

4.5. Comparison to observed fire activity

To broadly evaluate how well our estimates of wildfire potential align with observed fire activity, we compared our historical *maximum KBDI*$_{adj}$ to annual occurrence of fire based on the MODIS burned area product, as discussed in 3.5 *Evaluation of observed fire activity* of the *Methods* section. Although these two datasets evaluate different metrics and time periods (wildfire potential from 1975–2005 and frequency of fire occurrence from 2000–2020, respectively), this analysis allows us to identify general relationships between our modelled results and observed fire activity. Using a Spearman rank-order correlation, we find a moderately strong relationship between these two datasets across all land grid cells globally, with a correlation value of 0.61 ($P < 0.001$). While wildfire potential is representative of where fires could occur, this comparison indicates that our *maximum KBDI*$_{adj}$ value in the historical baseline broadly aligns with areas in which fires have occurred with regular frequency in the recent past.

5. Discussion

Through our evaluation of future wildfire potential, we find significant increases in both severity and frequency of conditions conducive to wildfire activity. Climate change and consequent warming and drying patterns are projected to elevate the potential for wildfires across all vegetated regions of the globe. We also find that even marginal changes in just one dimension of wildfire potential could create novel risks in historically wet and cool regions or increase the chances of severe wildfires in already wildfire-prone areas.

In Central and South America, as well as much of Africa, year-round high temperatures coupled with any period of reduced precipitation, for example as a result of drivers such as the El Niño-Southern Oscillation (Flannigan *et al* 2009), will quickly introduce levels of high wildfire potential. This is particularly the case for *maximum KBDI*$_{adj}$ at both mid- and end-of-century. We find broad agreement between our end-of-century results and those of Liu *et al* (2010), including the finding that areas with the highest relative increases in wildfire potential in the future are the same as those with large fire potential at present.

Many mid-latitude locations emerge with some of the highest *change in maximum KBDI*$_{adj}$ globally, places which may not necessarily have experienced a high frequency of wildfires historically. However, the dominant vegetation type is highly burnable and meteorological conditions are trending towards higher potential for wildfires. As a result, many of these communities may be less equipped to deal with wildfires and potentially be more vulnerable due to their lack of recent experience managing large-scale wildfire events. Additionally, the Amazon, with its exceptionally high volume of biomass, is a notable hotspot for future wildfire activity as the extent and severity of drought could significantly expand throughout the century (Duffy *et al* 2015). In addition to experiencing high KBDI, we find that the *number of high days*$_{adj}$ in the Amazon will significantly increase. This is in agreement with observational studies showing that the wildfire season has increased in length by over a month over the last 35 years (Jolly *et al* 2015). Longer wildfire seasons in the Amazon (figure 3(d)) could also increase the severity and frequency of runaway fires from agricultural and land-clearing activities, which would have an even greater impact on local biodiversity and global fire emissions.

Many mid- and upper-latitude regions, such as North America and Northern and Central Europe, are some of the places where the effects of climate change, namely rising temperatures and shifting precipitation patterns, will be disproportionately felt compared to the rest of the world. Although the current exposure to wildfires may be relatively low in some of these areas, they may become hotspots for risk over the course of the century. This exposure is particularly noticeable for *change in maximum KBDI*$_{adj}$, for instance in the Central Europe sub-region, where the conditions will be significantly more conducive to wildfires by the end of the century due in part to warming trends. For example, Brown *et al* (2020) found that warming is the main driver of higher KBDI values in North America due to that fact that relative temperature increases are generally higher and uniformly one-directional compared to precipitation changes.

Tropical regions have already experienced a rapid rise in both fire size and frequency in recent decades, in part due to land management practices (Flannigan *et al* 2009), a trend which seems likely to continue. Some of

the highest counts of *number of high days*$_{adj}$ could occur in the vegetation-dense areas of Australia, where recent wildfires demonstrated how dry periods can contribute to severe, widespread, and damaging wildfires. By the end of the century, the number of *high KBDI days*$_{adj}$ per year will be a significant threat to many regions around the world, as the frequency of days with high wildfire potential increases, elevating the chances that a large, destructive fire, or an exceptionally long fire season, could occur.

Like Liu *et al* (2010), we also find that some of the most pronounced shifts in wildfire potential are due to relative increases in high KBDI days, especially at mid-latitudes. At the foothills of the Himalayas, a significant increase in *number of high days*$_{adj}$ is projected to elevate wildfire potential for a larger portion of the year, likely overlapping with intentional agricultural fires that are usually ignited by local farmers between October and November (Jethva *et al* 2019). Populations in the western region of the United States are well acquainted with wildfires, which typically occur in late summer (September and October), but may have to contend with even larger fires earlier and later in the year as higher temperatures and extended dry periods build up fuel loads. As a result of prolonged wildfire seasons due to climate change, it may become necessary to extend fire bans to last a majority or the entirety of the year.

Extreme northern latitudes, such as parts of northern Canada and Russia, begin to exhibit some *high days*$_{adj}$ in mid- and end-of-century time periods. Although the wildfire seasons in the extreme north may not be as long as in other parts of the world, the combination of widely available burnable fuel sources and at least a few high-risk days indicate that under drier and hotter conditions, wildfires will be increasingly possible. This suggests that many regions which have low or moderate wildfire potential today could emerge as wildfire hotspots as early as mid-century.

6. Limitations

There are several notable limitations in our methodology. First and foremost, this is an assessment of *wildfire potential*, and addresses only at a high level the prevailing conditions which may allow for a wildfire to occur and expand. Whether or not a fire actually occurs, as well as the subsequent characteristics of a fire, depend on many discrete factors, including ignition source and certain local meteorological conditions such as humidity and wind, which are excluded from our analysis. No wildfire will occur without an ignition source, and yet a single spark can be enough to initiate a devastating wildfire under the right conditions. Ignition can be either natural or related to human activity, the exact source of which plays a critical role in the number of fire occurrences and area burned (Syphard and Keeley 2015). Additionally, some fires may be set intentionally (legally or illegally), whether for prescribed burns as part of wildfire mitigation programs (Fernandes and Botelho 2003), for agricultural purposes (McCarty *et al* 2007), or for clearing forests for pastures (Beck *et al* 2008). While set intentionally, these types of fires can become uncontrollable and evolve into a widespread wildfire, as may have been the case for wildfires in Brazil in 2019 (Hughes 2019). Our analysis does not attempt to account for various types of ignition sources and their associated degrees of uncertainty, instead focusing on where wildfires could occur based on prevailing meteorological drivers related to climate change and existing land cover types.

Within the components of our wildfire potential approach, several notable constraints also exist. Although our analysis extends through the end of the century, the ESA dataset is a point-in-time land cover classification from 2015. By the end of our analysis window, land cover will be altered in sometimes significant ways, not only from changes to land use, such as conversion of land to built environment or forest to pasture, but also from changes driven by climate change (IPCC 2019), for example desertification and shifting biomes. As such, our analysis reflects wildfire potential and the impacts of climate change based on 2015 land cover classifications and does not attempt to project changes in land cover over time. By evaluating the land types which burned in past wildfires, we carry forward land use histories and some of the meteorological effects which gave rise to observed fires. These historical observations are used to calculate the burnable coefficients, which may or may not be representative of the future.

As discussed in the *Methods* section, we assign binned weighting factors ranging from zero to one to each ESA CCI land cover classification (see the *Land Cover* section of the *supplementary materials*), based on composite normalized values of fire intensity from Kganyago and Shikwambana (2020) and of fire occurrence derived from the MODIS Burned Area product (Giglio *et al* 2018). This approach allows us to apply a burnable coefficient across the globe after upsampling to a ¼° resolution. However, there are several caveats in this approach. For fire intensity, Kganyago and Shikwambana (2020) evaluate only three regions of the globe: the western United States, Brazil, and eastern Australia. Furthermore, the analysis covers only two years, 2018 and 2019, years in which large, severe fires occurred in each of the analysis regions. Additionally, ESA land cover types are grouped and evaluated together, reducing the granularity of fire intensity associated to specific land cover types. As a result, the fire intensity component of our burnability weighting factor may not capture the full range of possible intensity values globally and over time, which is further locally dependent upon even more

discrete conditions. However, it provides us a method to broadly associate ESA CCI land cover classifications with maximum fire radiative power based on historical data. For fire occurrence, the MODIS Burned Area product may overrepresent the susceptibility of wildfires for particular land cover classifications, for instance in agricultural lands, where intentional fires set for crop management purposes count the same as a true wildfire. Finally, our approach to normalize, average, and bin each component of the burnability weighting factor ultimately reduces the precision of our results. Additionally, even within an individual land cover type, there are species-specific relationships with certain wildfire characteristics, such as severity (Rogers *et al* 2015), for which we cannot account. While our approach allows us to derive a single composite factor for burnability, we acknowledge that our results would change with a more refined land cover classification weighting scheme.

KBDI has some caveats of its own. Most notably, the index was developed in the southeastern United States, and thus reflects the relationship between evapotranspiration and vegetation dryness of this region. As a result, this formula may not necessarily hold up as well across the globe when evaluating different vegetation and soil types. These deficiencies are well documented, and other studies have made attempts to improve the KBDI equation (e.g., Taufik *et al* 2015). As a result, regions may not as accurately reflect the actual soil moisture deficit for a given region as compared to the southeast US. For example, Taufik *et al* (2017) found that KBDI performed better in tropical wetland ecosystems when accounting for water table depth. Localized water table and soil characterization data were not used in our analysis but could supplement future research of wildfire potential. Burning potential in fuel-limited ecosystems such as shrub and grasslands may be more correlated with antecedent precipitation rates, and generally, fuel productivity rather than fuel dryness. However, we elected to use fuel availability, and a metric more indicative of fuel dryness because the high(er) level of model agreement among GCMs when projecting more moderate levels of climatic changes. Fuel productivity, rather, relies heavily upon intra-seasonal estimates of precipitation spikes, the volumes of rainfall responsible for significant fuel build-up in grasslands and shrublands. Although a few GCMs may show significant changes in rainfall when attempting to simulate seasonal or intra-decal oscillations such as ENSO, the degree of model agreement in projecting such events (e.g., ENSO) remains low (Taschetto *et al* 2014, Chen *et al* 2017), and seasonal precipitation spikes are not evident when averaging across decades. Globally, fuel continuity and fuel dryness are the dominant factors of burnt area globally (Kelley *et al* 2019), which may generally suggest that our election to measure fuel availability and dryness allows for broader, global applications.

Additionally, our results are subject to the inherent limitations of climate models. Model simulations, including the downscaled product of the CMIP5 generation climate models used in our analysis, are imperfect tools and may perform relatively better or worse in certain regions and timeframes (Flato *et al* 2013). Extreme precipitation anomalies such as drought may not always be well captured in the GCMs (Dai 2006, Kendon *et al* 2012), leading to underrepresentation of risks in some areas. In northern latitudes, for example, the alignment of prolonged drying patterns and extreme temperatures could produce severe wildfires. Our results are the multi-model mean of an 18-model ensemble, which attempts to limit biases from individual models, but does not resolve systematic biases present across all GCMs (Knutti *et al* 2010), nor does it represent the full range of variability present across models.

7. Conclusion

Our analysis evaluates future wildfire potential globally, using KBDI and land cover classifications to represent climatological conditions related to wildfires and the availability of burnable fuel sources, respectively. Through analysis of both severity and frequency of wildfire potential, we find the absolute and relative dimensions of wildfire potential are projected to increase, to varying degrees, across the entire globe. Tropical regions emerge as hotspots, where an abundance of burnable land cover combined with rising temperatures and changing precipitation patterns elevate the wildfire potential maximum severity. Many mid- and high-latitude regions will also experience significant increases in wildfire potential, particularly by the end-of-century. For most regions, the additional number of high wildfire potential days in a season is estimated to increase, signaling an urgent need for local authorities to heavily invest in wildfire prevention and mitigation strategies throughout the year. While wildfires may still be rare occurrences in many places globally, we find that shifting patterns of temperature and precipitation driven by climate change are increasing wildfire potential across the board. As a result, these patterns are likely to create new levels of risk and challenge efforts to effectively manage forest systems and protect communities across the globe.

Acknowledgments

Access and usage of the downscaled climate and land cover data was possible due to the efforts and public-facing missions of the Coupled Model Intercomparison Project, NASA Earth Exchange Global Daily Downscaled

Projections and MODIS projects, and the European Space Agency Land Cover Climate Change Initiative. We also thank our frequent collaborators and fellow researchers at Four Twenty Seven, Josh Turner, John Naviaux, and Natalie Ambrosio Preudhomme. Their insights and thoughtful feedback helped improve this manuscript.

Data availability statement

The data that support the findings of this study are available upon reasonable request from the authors.

ORCID iDs

Colin S Gannon https://orcid.org/0000-0002-5608-2768
Nik C Steinberg https://orcid.org/0000-0002-2717-4807

References

Abatzoglou J T and Kolden C A 2013 Relationships between climate and macroscale area burned in the western United States *International Journal of Wildland Fire* **22** 1003–20
Abatzoglou J T and Williams A P 2016 Impact of anthropogenic climate change on wildfire across western US forests *PNAS* **113** 11770–5
Ainuddin N A and Ampun J 2008 Temporal analysis of the keetch-byram drought index in Malaysia: implications for forest fire management *Journal of Applied Sciences* **8** 3991–4
Beck E, Hartig K and Roos K 2008 Forest clearing by slash and burn *Gradients in a Tropical Mountain Ecosystem of Ecuador* (Berlin Heidelberg: Springer) pp 371–4
Bowman D M J S *et al* 2009 Fire in the earth system *Science* **324** 481–4
Brown T J, Hall B L and Westerling A L 2004 The impact of twenty-first century climate change on wildland fire danger in the western united states: an applications perspective *Clim. Change* **62** 365–88
Brown E K, Wang J and Feng Y 2020 U.S. wildfire potential: a historical view and future projection using high-resolution climate data *Environmental Research Letters* **in press** 1–24
Burgan R E, Klaver R W and Klaver J M 1998 Fuel models and fire potential from satellite and surface observations *International Journal of Wildland Fire* **8** 159–70
Chen C, Cane M A, Wittenberg A T and Chen D 2017 ENSO in the CMIP5 simulations: life cycles, diversity, and responses to climate change *J. Clim.* **30** 775–801
Chu P-S, Yan W and Fujioka F 2002 Fire-climate relationships and long-lead seasonal wildfire prediction for Hawaii *International Journal of Wildland Fire* **11** 25–31
Cochrane M A and Ryan K C 2009 Fire and fire ecology: concepts and principles *Tropical Fire Ecology* (Berlin, Heidelberg: Springer) pp 25–62
Coogan S C P, Robinne F N, Jain P and Flannigan M D 2019 Scientists' warning on wildfire—a Canadian perspective *Can. J. For. Res.* **49** 1015–23
Cook B I, Ault T R and Smerdon J E 2015 Unprecedented 21st century drought risk in the American Southwest and Central Plains *Sci. Adv.* **1** 1–8
Dai A 2006 Precipitation characteristics in eighteen coupled climate models *J. Clim.* **19** 4605–30
Dillon G K, Menakis J and Fay F 2015 Wildland fire potential: A tool for assessing wildfire risk and fuels management needs *Proceedings of the large wildland fires conference (Missoula, MT, May 19-23, 2014)* (Fort Collins, CO: U.S. Department of Agriculture, Forest Service, Rocky Mountain Research Station) 60–76 (https://fs.usda.gov/treesearch/pubs/all/49429)
Dimitrakopoulos A P and Bemmerzouk A M 1998 Evaluation of the Canadian forest fire danger rating system (CFFDRS) and the Keetch-Byram index (KBDI) in the Mediterranean climate of Greece *Proc. of III Int. Conf. on Forest Fire Research 14th Conf. on Fire and Forest Meteorology*
Dimitrakopoulos A P and Bemmerzouk A M 2003 Predicting live herbaceous moisture content from a seasonal drought index *Int. J. Biometeorol.* **47** 73–9
Dimitrakopoulos A P, Mitsopoulos I D and Gatoulas K 2010 Assessing ignition probability and moisture of extinction in a Mediterranean grass fuel *International Journal of Wildland Fire* **19** 29–34
Dolling K, Chu P S and Fujioka F 2009 Natural variability of the Keetch–Byram drought index in the Hawaiian Islands *International Journal of Wildland Fire* **18** 459–75
Duffy P B, Brando P, Asner G P and Field C B 2015 Projections of future meteorological drought and wet periods in the Amazon *PNAS* **112** 13172–7
ESA 2017 Land Cover CCI Product User Guide Version 2. Tech. Rep. Retrieved February 24, 2020 from (http://maps.elie.ucl.ac.be/CCI/viewer/download/ESACCI-LC-Ph2-PUGv2_2.0.pdf)
Fernandes P M and Botelho H S 2003 A review of prescribed burning effectiveness in fire hazard reduction *International Journal of Wildland Fire* **12** 117–28
Finkele K, Mills G A, Beard G and Jones D A 2006 National gridded drought factors and comparison of two soil moisture deficit formulations used in prediction of Forest Fire Danger Index in Australia *Aust. Meteorol. Mag.* **55** 183–97
Flannigan M D, Krawchuk M A, De Groot W J, Wotton B M and Gowman L M 2009 Implications of changing climate for global wildland fire *International Journal of Wildland Fire* **18** 483–507
Flato G *et al* 2013 Evaluation of climate models *Climate Change 2013 the Physical Science Basis: Working Group I Contribution to the Fifth Assessment Report of the Intergovernmental Panel on Climate Change* 741–866
Forkel M *et al* 2019 Emergent relationships with respect to burned area in global satellite observations and fire-enabled vegetation models *Biogeosciences* **16** 57–76
French C 2020 America on fire: climate change, wildfires & insuring natural catastrophes *UC Davis Law Review* **54** 817–85
Ganatsas P, Antonis M and Marianthi T 2011 Development of an adapted empirical drought index to the Mediterranean conditions for use in forestry *Agric. For. Meteorol.* **151** 241–50

Garcia-Prats A, Antonio D C, Tarcísio F J G and Antonio M J 2015 Development of a Keetch and Byram-Based drought index sensitive to forest management in Mediterranean conditions *Agric. For. Meteorol.* **205** 40–50
Giglio L, Boschetti L, Roy D P, Humber M L and Justice C O 2018 The collection 6 MODIS burned area mapping algorithm and product *Remote Sens. Environ.* **217** 72–85
Gillett N P, Weaver A J, Zwiers F W and Flannigan M D 2004 Detecting the effect of climate change on Canadian forest fires *Geophysical Research Letters* **31** L18211
Goss M, Swain D L, Abatzoglou J T, Sarhadi A, Kolden C, Williams A P and Diffenbaugh N S 2020 Climate change is increasing the risk of extreme autumn wildfire conditions across California *Environ. Res. Lett.* **15** 094016
Herring S C *et al* 2018 Explaining Extreme Events of 2016 from a Climate Perspective *Bulletin of the American Meteorological Society* **99** S1–S157
Hughes R 2019 *Amazon fires: What's the latest in Brazil?* (BBC News) (https://bbc.com/news/world-latin-america-49971563)
IPCC 2019 *Climate Change and Land: an IPCC Special Report on Climate Change, desertification, land Degradation, Sustainable land Management, Food Security, and Greenhouse Gas Fluxes in Terrestrial Ecosystems* (https://ipcc.ch/srccl/)
Iturbide M *et al* 2020 An update of IPCC climate reference regions for subcontinental analysis of climate model data: definition and aggregated datasets *Earth System Science Data* **12** 2959–70
Jethva H, Torres O, Field R D, Lyapustin A, Gautam R and Kayetha V 2019 Connecting crop productivity, residue fires, and air quality over Northern India *Sci. Rep.* **9** 1–11
Johnson M B and Forthum G 2001 Spatial mapping of KBDI for the southeast United States *Proc. of the 4th Symp. on Fire and Forest Meteorology (Nevada)* (American Meteorological Society, Preprints) pp 13–5
Jolly W M, Cochrane M A, Freeborn P H, Holden Z A, Brown T J, Williamson G J and Bowman D M J S 2015 Climate-induced variations in global wildfire danger from 1979 to 2013 *Nat. Commun.* **6** 1–11
Keetch J J and Byram G M 1968 A drought index for forest fire control *US Department of Agriculture, Forest Service, Southeastern Forest Experiment Station* **38** 1–32
Kelley D I, Bistinas I, Whitley R, Burton C, Marthews T R and Dong N 2019 How contemporary bioclimatic and human controls change global fire regimes *Nat. Clim. Change* **9** 690–6
Kendon E J, Roberts N M, Senior C A and Roberts M J 2012 Realism of rainfall in a very high-resolution regional climate model *J. Clim.* **25** 5791–806
Kganyago M and Shikwambana L 2020 Assessment of the characteristics of recent major wildfires in the USA, Australia and Brazil in 2018-2019 using multi-source satellite products *Remote Sensing* **12**
Kitzberger T, Falk D A, Westerling A L and Swetnam T W 2017 Direct and indirect climate controls predict heterogeneous early-mid 21st century wildfire burned area across western and boreal North America *PLoS One* **12** 1–24
Kirchmeier-Young M C, Zwiers F W, Gillett N P and Cannon A J 2017 Attributing extreme fire risk in Western Canada to human emissions *Climatic Change* **144** 365–79
Knutti R, Furrer R, Tebaldi C, Cermak J and Meehl G A 2010 Challenges in combining projections from multiple climate models *J. Clim.* **23** 2739–58
Li Z, Cihlar J and Nadon S 2000 Satellite-based detection of Canadian Boreal forest fires: development and application of the algorithm *Int. J. Remote Sens.* **21** 3057–69
Limaye V S, Max W, Constible J and Knowlton K 2019 Estimating health-related costs of ten US climate-sensitive events in 2012: a retrospective study *The Lancet Planetary Health* **3** S5
Liu Y, Stanturf J and Goodrick S 2010 Trends in global wildfire potential in a changing climate *Forest Ecology and Management* **259** 685–97
van Mantgem P J *et al* 2009 Widespread increase of tree mortality rates in the western United States *Science* **323** 521–4
McCarty J L, Justice C O and Korontzi S 2007 Agricultural burning in the Southeastern United States detected by MODIS *Remote Sens. Environ.* **108** 151–62
Mitri G, Jazi M and McWethy D 2015 Assessment of wildfire risk in Lebanon using geographic object-based image analysis *Photogrammetric Engineering & Remote Sensing* **81** 499–506
Partain J L *et al* 2016 An Assessment of the Role of Anthropogenic Climate Change in the Alaska Fire Season of 2015 *Bulletin of the American Meteorological Society* **97** S14–8
Paysen T E, Ansley R J, Brown J K, Gotffried G J, Haase S M, Harrington M G, Narog M G, Sackett S S and Wilson R C 2000 Chapter 6: fire in Western Shrubland, woodland, and grassland ecosystems *Wildland Fire and Ecosystems: Effects of Fire on Flora. Ogden (UT): US Department of Agriculture Forest Service, Rocky Mountain Research Station. General Technical Report RMRS-GTR-412-vol* **2** 121–59
Pechony O and Shindell D T 2010 Driving forces of global wildfires over the past millennium and the forthcoming century *PNAS* **107** 19167–70
Pellizzaro G, Duce P, Ventura A and Zara P 2007 Seasonal variations of live moisture content and ignitability in shrubs of the Mediterranean Basin *International Journal of Wildland Fire* **16** 633–41
Roads J, Fujioka F, Chen S and Burgan R 2005 Seasonal fire danger forecasts for the USA *International Journal of Wildland Fire* **14** 1–18
Rogers B M, Soja A J, Goulden M L and Randerson J T 2015 Influence of tree species on continental differences in boreal fires and climate feedbacks *Nat. Geosci.* **8** 228–34
Short K C 2014 A spatial database of wildfires in the United States, 1992–2011 *Earth System Science Data* **6** 1–27
Sommers W T, Coloff S G and Conard S G 2011 Synthesis of knowledge: fire history and climate change *JFSP Synthesis Reports. Paper 19* p 190 (http://firescience.gov/JFSP_fire_history.cfm)
Stephenson N 1998 Actual evapotranspiration and deficit: biologically meaningful correlates of vegetation distribution across spatial scales *Journal of Biogeography* **25** 855–70
Syphard A D and Keeley J E 2015 Location, timing and extent of wildfire vary by cause of ignition *International Journal of Wildland Fire* **24** 37–47
Taschetto A S, Sen Gupta A, Jourdain N C, Santoso A, Ummenhofer C C and England M H 2014 Cold tongue and warm pool ENSO events in CMIP5: mean state and future projections *J. Clim.* **27** 2861–85
Taufik M, Setiawan B I and van Lanen H A J 2015 Modification of a fire drought index for tropical wetland ecosystems by including water table depth *Agric. For. Meteorol.* **203** 1–10
Taufik M, Torfs P J J F, Uijlenhoet R, Jones P D, Murdiyarso D and Van Lanen H A J 2017 Amplification of wildfire area burnt by hydrological drought in the humid tropics *Nat. Clim. Change* **7** 428–31
Thompson MP and Calkin D E 2011 Uncertainty and risk in wildland fire management: A review *Journal of Environmental Management* **92** 1895–909
Thompson J R and Spies T A 2009 Vegetation and weather explain variation in crown damage within a large mixed-severity wildfire *Forest Ecology and Management* **258** 1684–94

Thrasher B L, Maurer E P, McKellar C and Duffy P B 2012 Technical Note: bias correcting climate model simulated daily temperature extremes with quantile mapping *Hydrol. Earth Syst. Sci. Discuss.* **9** 5515–29
Verbesselt J, Jonsson P, Lhermitte S, Van Aardt J and Coppin P 2006 Evaluating satellite and climate data-derived indices as fire risk indicators in savanna ecosystems *IEEE Trans. Geosci. Remote Sens.* **44** 1622–32
van Vuuren D P *et al* 2011 The representative concentration pathways: an overview *Clim. Change* **109** 5–31
Wahlberg M M, Triepke F J, Robbie W A, Stringer S H, Vandendriesche D, Muldavin E H and Malusa J R 2014 Ecological response units of the Southwestern United States *U.S. Forest Service, Southwest Region* **FR-R3-XX-XX** 201
Westerling A L, Hidalgo H G, Cayan D R and Swetnam T W 2006 Warming and earlier spring increase Western U.S. forest wildfire activity *Science* **313** 940–3
Williams A P, Abatzoglou J T, Gershunov A, Guzman-Morales J, Bishop D A, Balch J K and Lettenmaier D P 2019 Observed impacts of anthropogenic climate change on wildfire in California *Earth's Future* **7** 892–910
Xanthopoulos G, Maheras G, Gouma V and Gouvas M 2006 Is the Keetch-Byram drought index (KBDI) directly related to plant water stress? *Forest Ecology and Management* **234** S27
Yoon J H, Kravitz B, Rasch P J, Simon Wang S Y, Gillies R R and Hipps L 2015 Extreme fire season in California: a glimpse into the future? *Bull. Am. Meteorol. Soc.* **96** S5–9